Boundary-Layer Meteorol (2007)

ORIGINAL PAPER

Local scales of turbulence in the stable boundary layer

Zbigniew Sorbjan[1]

Submitted on 19 July 2007, accepted on 15 December 2007

Abstract Local, gradient-based scales, which contain the vertical velocity and temperature variances, as well as the potential temperature gradient, but do not include fluxes, are tested using data collected during the CASES-99 experiment. The observations show that the scaling based on the temperature variance produces relatively smaller scatter of empirical points. The resulting dimensionless statistical moments approach constant values for sufficiently large values of the Richardson number Ri. This allows one to derive predictions for the Monin-Obukhov similarity functions φ_m and φ_h, the Prandtl number Pr, and the flux Richardson number Rf in weak turbulence regime.

Keywords: Gradient-based scaling, Local scaling, Similarity theory, Stable boundary layer

[1] Z.Sorbjan,
Department of Physics, Marquette University,
Milwaukee, WI 53201-1881, USA, e-mail: sorbjanz@mu.edu

1 Introduction

Observations show that the stable boundary layer (SBL) at night overland has a very complex and variable structure (e.g., Poulos et al. 2002, Grachev et al 2007a, b). Its adequate description depends on high-resolution measurements. Nocturnal turbulence is often confined to thin layers, sometimes less than 1 m deep (Chimonas 1999; Poulos and Burns 2003; Balsley et al. 2003). The stable boundary layer requires careful calculation of turbulence quantities (e.g., Mahrt and Vickers 2006). The conventional methods for computing turbulent moments within very weak turbulence are usually insufficient, due to the effects of mesoscale motions and large random errors. The SBL is controlled by a variety of factors, such as wind shear, wind meandering, wavelike motions, radiative cooling (e.g., Garratt and Brost 1981; Ha and Mahrt 2003), phase changes (e.g., Duynkereke 1999), nonstationarity, advection, subsidence, and topography (e.g., Brost and Wyngaard 1978; Derbyshire and Woods 1994; Mahrt 2007). Its depth might not be well defined (e.g., Mahrt et al. 1998).

The SBL can be categorized as turbulent, intermittent, and radiative (Van de Wiel et al. 2003), or classified into either weakly or very stable regimes (Mahli 1995; Oyha et al. 1997; Mahrt et al. 1998). The weakly stable regime is characterized with a sub-critical Richardson number *Ri*, significant wind shear, clouds, and continuous turbulence near the surface. In contrast, the very stable regime is characterized by small wind shear, clear skies, overcritical values of *Ri*, and intermittent turbulence. The very stable regime often has an "upside-down" character, with the strongest turbulence at the top of the surface inversion layer, where it is generated by vertical shear on the underside of the lower-level jet stream. The upper portion of the SBL can be detached from the nearly laminar surface sub-layer. The detachment may be temporary, since flow acceleration above the very stable surface layer may lead to shear generation of turbulence and re-coupling of elevated turbulence with the surface (Businger, 1973).

Currently, there is no preferred similarity theory that would adequately treat all the described properties of the SBL. Each of the existing theories has limitations. The surface-layer similarity (Monin-Obukhov 1954) is confirmed only in cases with strong, continuous turbulence, when the gradient Richardson number *Ri* is constant and sub-critical. In cases when the Richardson number is outside of the critical limit, the "z-less" predictions of “flux-based”

similarity functions are invalid (Sorbjan 2006c), and strongly affected by self-correlation (Klipp and Mahrt 2004). Nieuwstadt's (1984) local theory, based on "flux-based" local scaling, is valid only during continuous, quazi-steady turbulence, for which the heat flux variation is nearly linear with height. Its local extension (e.g., Sorbjan 1995), in which the fluxes are allowed to be non-linear with height, is more general, but it also lacks consistency, when the Richardson number varies with height, and also when it is outside of its critical limit.

In an attempt to overcome the described drawbacks, Sorbjan (2006a, b) proposed the "gradient-based" local scaling, based on the vertical velocity variance σ_w^2. Such scaling, however, is not unique in stable conditions, and other scales of turbulence can also be formed (Sorbjan 2007a). They can be based on various moments of turbulence, such as the potential temperature variance σ_θ^2 (which leads to the Ellison length scale), or the viscous dissipation ε (which yields the Ozmidov scale).

The purpose of the present sudy is to further explore the local similarity approach by analyzing alternate scaling systems. The article focuses on scales constructed on the basis of the vertical velocity and temperature variances, and has the following structure. Local scaling is briefly reviewed and discussed in Section 2. In Section 3, both types of scales are examined, based on composite data obtained during the CASES-99 field experiment. Final remarks are presented in Section 4.

2 Local scaling

Nieuwstadt (1984) considered a system of seven dry, steady-state, second-order moment equations, modified by the additional assumptions that the stress, the velocity gradient, and the horizontal heat flux are parallel. The set included equations for the turbulent kinetic energy E, the vertical velocity variance $\overline{w^2}$, the modulus of the Reynolds stress $\tau = \left[\overline{uw}^2 + \overline{vw}^2\right]^{1/2}$, the vertical heat flux $\overline{w\theta}$, the horizontal heat flux $H = \left[\overline{u\theta}^2 + \overline{v\theta}^2\right]^{1/2}$, and the temperature variance $\overline{\theta^2}$. Employing the local Monin-Obukhov scales:

$$\Lambda_*(z) = -\tau^{3/2}/(\kappa\beta\overline{w\theta}), \qquad U_*(z) = \tau^{1/2}, \qquad T_*(z) = -\overline{w\theta}/\tau^{1/2} \tag{1}$$

where κ is the von Karman constant, $\beta = g/T_o$ is the buoyancy parameter, and assuming that the mixing length l is linear with height, allowed him to obtain the system of equations, which contained dimensional combinations: $K_M/U_*\Lambda_*$, $K_H/U_*\Lambda_*$, $\overline{w^2}/U_*^2$, E/U_*^2, H/U_*T_*, $\overline{w\theta}/U_*T_*$, $\overline{\theta^2}/T_*$, and z/Λ_*, where K_M and K_H are the eddy viscosity and diffusivity. In the limit of $z/\Lambda_* \rightarrow \infty$, the equations no longer contained z as a variable (the "z-less" regime), and as a consequence, the listed dimensionless quantities could be expected to approach constant values.

The result can be generalized by a statement that a statistical moment X in the SBL, scaled in terms of (1), is expected to be dependent on the dimensionless height z/Λ_* (Sorbjan 1995). The dimensionless moment approaches a constant value for sufficiently large values of z/Λ_*, which is referred to as the "z-less regime":

$$\frac{X}{U_*^a T_*^a \Lambda_*^a} = f(\frac{z}{\Lambda_*}) \rightarrow const \qquad (2)$$

for $z/\Lambda_* \rightarrow \infty$, where a, b, and c are appropriate power coefficients. The above expression implies that the gradient Richardson number $Ri = N^2/S^2 \propto (\beta T_*/\Lambda_*)/(U_*/\Lambda_*)^2 = const$, where $N = (\beta\, d\Theta/dz)^{0.5}$ is the Brunt-Väisälä frequency, and $S = \left[\left(dU/dz\right)^2 + \left(dV/dz\right)^2\right]^{1/2}$ is the wind shear. Note that the potential temperature Θ in the definition of the Brunt-Väisälä frequency must be monotonic with height, and its vertical gradient positive. The monotonic profile can be obtained by time averaging in cases of coarse vertical measurements (Mahrt and Vicker 2006), or by adiabatic sorting in cases of fine vertical measurements (Sorbjan and Balsley 2007, in preparation).

The hypothesis (2) was found to be valid for gradients, variances, covariances, eddy viscosities and diffusivities, dissipation rates, structure parameters C_v^2, C_T^2, spectra and cospectra, but only in the continuous, sub-critical case (Sorbjan 1995). In the intermittent case near the Earth's surface, however, when $\overline{w'\theta'} \sim 0$, $\overline{u'w'} \sim 0$, the similarity predictions fail as the temperature gradient cannot be accurately defined based on fluxes: $d\Theta/dz \propto T_*/\Lambda_* \propto$

$\beta\ \overline{w\theta}^2/\overline{u'w'}$ and is indetermined.

Sorbjan (2006a, b) argued that when fluxes in the stable regime are small, they must be remoed from the list of governing parameters. The similarity scales should be based on scalar gradients, which lead to the following set of local (height dependent), gradient-based scales for length, velocity and temperature:

$$L_w(z) = \sigma_w/N, \qquad U_w(z) = \sigma_w, \qquad T_w(z) = \sigma_w N/\beta \tag{3}$$

where $\sigma_w^2 = \overline{w^2}$ is the vertical velocity variance.

The master length scale L_w corresponds to the vertical distance by which a parcel of air moves, when its kinetic energy is converted to work against the buoyancy force. It can be derived by equating the production and dissipation terms in the turbulent energy equation.

Applying the scales (3) to Nieuwstadt's second-order moment equations, together with a closure assumption that the mixing length l is linear wih height, leads to the conclusion that the dimensional combinations in the resulting set of equations depend only on the dimensionless parameter z/L_w (Sorbjan 2006a), namely:

$$Ri \propto \overline{w\theta}/(U_w T_w) \propto H/(U_w T_w) \propto \overline{\theta^2}/T_w^2 \propto e^2/U_w^2 \propto \tau/U_w^2 = f(z/L_w) \tag{4}$$

Note that (4) implies that $Ri = f(z/L_w)$. As a result, (4) can be rewritten in an alternative form:

$$\overline{w\theta}/(U_w T_w) \propto H/(U_w T_w) \propto \overline{\theta^2}/T_w^2 \propto e^2/U_w^2 \propto \tau/U_w^2 = f(Ri) \tag{5}$$

The obtained result can be generalized, based on similarity theory arguments, by stating that a statistical moment X in the SBL, scaled in terms of (4), is expected to be a function of a local Richardson number Ri (Sorbjan, 2006a):

$$\frac{X}{U_w^a T_w^b L_w^c} = f(Ri) \tag{6}$$

where *a, b,* and *c* are appropriate power coefficients.

An analogous procedure can be applied for the following set of scales:

$$L_\theta(z) = \beta\sigma_\theta/N^2, \quad T_\theta(z) = \sigma_\theta, \quad U_\theta(z) = \beta\sigma_\theta/N \tag{7}$$

where the master length scale L_θ indicates the mean size of eddies generated by temperature fluctuations in the stably stratified flow. The scale can be derived by equating the production and dissipation terms in the temperature variance equation.

From Nieuwstadt's equations, augmented by a closure assumption that the mixing length *l* is linear is linear with height, and Eq. (7), a system of dimensionless equations can obtained, analogous to the one obtained by Sorbjan (2006). The system indicates that all dimensional combinations depend on the dimensionless parameter z/L_θ:

$$Ri \propto \overline{w\theta}/(U_\theta T_\theta) \propto H/(U_\theta T_\theta) \propto \overline{\theta^2}/T_\theta^2 \propto E/U_\theta^2 \propto \tau/U_\theta^2 = f(z/L_\theta) \tag{8}$$

and as before, the above statement can be rewritten in an alternative form:

$$\overline{w\theta}/(U_\theta T_\theta) \propto H/(U_\theta T_\theta) \propto \overline{\theta^2}/T_\theta^2 \propto E/U_\theta^2 \propto \tau/U_\theta^2 = f(Ri) \tag{9}$$

The above result can be generalized by stating that a statistical moment *X* in the SBL, scaled in terms of (7), is expected to be a function of a local Richardson number *Ri*:

$$\frac{X}{U_\theta^a T_\theta^b L_\theta^c} = f(Ri) \tag{10}$$

where *a, b,* and *c* are appropriate power coefficients.

Expressing the similarity functions *f(Ri),* in (6) and in (10), in terms of the Richardson number *Ri* reduces the problem of self-correlation (Klipp and Mahrt 2004; Sorbjan 2006). In the

"gradient-based" formulation, self-correlation can only be caused by the Brunt-Väisälä frequency N. If a similarity function $f \sim N^a$, where a is a power coefficient (for example, $a = +1$ for the dimensionless temperature flux $\frac{\overline{w\theta}}{U_\theta T_\theta}$), is plotted against $Ri \sim N$, and a random error of N is δN, then one can expect that the "polluted" value f_p of f is: $f_p \sim N^a(1+\delta N/N)^a$, while the "polluted" value Ri_p of Ri is: $Ri_p \sim N(1+\delta N/N)$. In the considered example, if $\delta N/N = 0.1$, and $a = +1$, an arbitrary point $[Ri_o, f(Ri_o)]$ will be shifted to a new position $[1.1\ Ri_o, 1.1\ f(Ri_o)]$. As a result, self-correlation will produce a linear dependence between $f(Ri)$ and Ri. The self-correlation effect can be quite severe within the Monin-Obukhov formulation, for parameters such as u_* and T_*, which are small in very stable conditions (so their relative errors are large). In the case of the Brunt-Väisälä frequency, the relative error $\delta N/N$ is expected to increase with height.

3 Empirical verification

The scaling set (3), was first tested by Sorbjan (2006a) by employing two composite cases described by Mahrt and Vickers (2006), and obtained from the CASES-99 observaions. The cases can be referred to as *W* (weak turbulence) and *S* (strong turbulence). Case *W* was characterized by a larger temperature difference between the bottom and the top of the tower at 60 m, smaller wind velocity. The Richardson number exceeded the critical value and the surface heat flux was relatively small. In Case *S*, the temperature difference between the top and the bottom of the tower was smaller than in case *W*, the wind speed greater, which produced stronger turbulence. The Richardson number was below the critical value, and the surface heat flux was larger than in Case *W*.

The same two composite cases *W* and *S* are considered herein. The resulting vertical profiles of scales (3) and (7) are shown in Figs. 1 a-c. The figures indicate that the scales are relatively smooth and nearly parallel. Both length scales L_w and L_θ are in the range of 2 – 16.5 m in Case *S*, and in the range of 0.3 - 0.9 m in Case *W*. The values of the length scales L_w and L_θ in

Case *W* are by one order of magnitude smaller than in Case *S*. The temperature scales T_w and T_θ are in the range of 0.25-0.8 K in Case *S*, and in the range of 0.05- 0.2 K in Case *W*. The velocity scales U_w and U_θ are in the range of 0.1–0.5 ms^{-1} in Case *S*, and in the range of 0.03-0.05 ms^{-1} in Case *W*. Generally, $L_w > L_\theta$, $T_w > T_\theta$, $U_w > U_\theta$ in the turbulent Case *S*. In case *W*, the scales are comparable, $L_w \approx L_\theta$, $T_w \approx T_\theta$, $U_w \approx U_\theta$.

The length scales increase with height in both cases *W* and *S*. The temperature scales decrease with height in both cases, and the velocity scales increase in Case *S* and decrease in case *W*. This can be explained by the fact that the Brunt-Väisälä frequency *N* decreases with height, from about 0.15 to 0.03 s^{-1} in case *W*, and from about 0.07 to 0.028 s^{-1} in case *S*. Note that the values of σ_θ (which is equal to T_θ) and σ_w (which is equal to U_w) are shown in Figures 1b and 1c. This allows verification that in case *S*, L_θ increases, because σ_θ is nearly constant and *N* decreases with height.

The dimensionless moments, scaled by (3) and (7), are shown in Figs. 2a-c as functions of the Richardson number. Note that data points obtained in Case *S* (black circles or squares) are located at sub-critical values of the Richardson number ($Ri < 0.25$), while for points obtained in Case W (grey circles and squares) the values of *Ri* are over-critical.

The dimensionless temperature flux $\overline{w\theta}/(U_W T_W)$ decreases in Fig. 2a, for decreasing values of the Richardson number. On the other hand, the dimensionless temperature flux decreases for larger values of *Ri*. At some value of *Ri,* between these two limiting regimes, which is about 0.25 in the figure, the dimensionless temperature flux reaches a minimum, equal to roughly -0.3. The presence of the minimum indicates that the value of the temperature flux in the SBL is bounded (Sorbjan, 2006). On the other hand, the dimensionless flux $\overline{w\theta}/(U_\theta T_\theta)$, in the figure, monotonically increases with *Ri*, from -1.1 for $Ri \approx 0.01$, and seems to be constant, equal to about -0.16 for $Ri > 1$. Scaling (7) does not produce the analogous minimum due to the fact that the product $U_\theta T_\theta$ increases with height in Case *S* (as it follows from Fig. 1).

The dimensionless momentum fluxes $\overline{uw}/U_W^2$ and $\overline{uw}/U_\theta^2$ are shown in Fig. 2b. The dimensionless flux $\overline{uw}/U_W^2$ monotonically increases toward zero with increasing the Richardson

number. The dimensionless flux $\overline{uw}/U_\theta^2$ in the figure monotonically increases with Ri, from the value of about -5.5 for $Ri \approx 0.01$, and seems to be constant, equal to about -0.2, for Ri > 1.

The dimensionless temperature variance $\overline{\theta^2}/T_w^2$ is shown in Fig. 2c. The dimensionless variance increases with increasing the Richardson number, and its values are significantly scattered for $Ri > 1$. The dimensionless vertical velocity variance $\overline{w^2}/U_\theta^2$ increases with increasing Ri and is approximately equal to 0.9 for $Ri > 1$.

The values of moments scaled by (7) in Figs. 2a-c can be divided into three zones. In the first zone $Ri < 0.25$. The second zone is a smooth transition to the third zone, where $Ri > 1$ and the dimensionless moments reach constant values:

$$\begin{aligned} \overline{w\theta} &\approx -0.15 U_\theta T_\theta = -0.15 \frac{\beta \sigma_\theta^2}{N} \\ \overline{uw} &\approx -0.2 U_\theta^2 = -0.2 \frac{\beta^2 \sigma_\theta^2}{N^2} \\ \overline{w^2} &\approx 0.9 U_\theta^2 = 0.9 \frac{\beta^2 \sigma_\theta^2}{N^2} \end{aligned} \qquad (11)$$

Based on the above result, the Monin-Obukhov similarity functions φ_m, φ_h, the Prandtl and flux Richardson numbers, Pr and Rf, can be written for $Ri > 1$ in the form:

$$\varphi_m = \frac{\kappa z}{\sqrt{-\overline{uw}}} S = \frac{\kappa}{\sqrt{0.2}} \frac{1}{Ri^{1/2}} \frac{z}{L_\theta} = 0.9 \frac{F_L(Ri)}{Ri^{1/2}} \qquad (12a)$$

$$\varphi_h = \kappa z \frac{\sqrt{-\overline{uw}}}{\overline{w\theta}} \frac{N^2}{\beta} = \kappa \frac{\sqrt{0.2}}{0.15} \frac{z}{L_\theta} \sim 1.2 F_L(Ri) \qquad (12b)$$

$$Pr = \frac{\varphi_h}{\varphi_m} = 1.3 Ri^{0.5} \qquad (12c)$$

$$Rf = \frac{\beta \overline{w\theta}}{\overline{uw}\, S} = 0.75 Ri^{0.5} \qquad (12d)$$

where $z/L_\theta = F_L(Ri)$. The expression for F_L for $Ri > 1$ can be obtained based on Fig. 7 in the

form for $z/L_\theta = aRi^b + c$, where *a, b* and *c* are constants, and *b* is presumably between 0.5 and 1. The function F_L is plotted in Fig. 7 with $a = 25$, $c = 0$, and $b = 0.6$ in the range of *Ri* from 1 to 6. As a result, $\varphi_m \sim Ri^{0.1}$ and $\varphi_h \sim Ri^{0.6}$. For the same values of constants, Eqs. (12c) and (12d) yield $Pr = 1.3$ and $Rf = 0.75$ for $Ri = 1$, and $Pr = 3.18$ and $Rf = 1.18$ for $Ri = 6$.

Note that the function φ_m in (12a) increases more slowly with *Ri* than φ_h in (12b). This conclusion differs from the result obtained by Grachev et al (2007a), and displayed as a function of both the dimensionless Monin-Obukhov height $\zeta = z/L$, and the bulk Richardson number Ri_B. However, a simple analysis indicates that ratios of small quantities $\frac{S}{\sqrt{-\overline{uw}}}$ and $\frac{\sqrt{-\overline{uw}}}{\overline{w\theta}}N^2$ in the definitions of φ_m and φ_h ensure that empirical similarity functions in very weak turbulence can be affected by substantial errors. Moreover, self-correlation in Eq. (12a) is linear with respect to *S*, and quadratic on both axes with respect to *N* in Eq. (12b). Consequently, the effects of self-correlation are expected to be stronger for $\varphi_h(Ri)$ than for $\varphi_m(Ri)$. It is worth emphasizing that φ_m will not be affected by self-similarity, when plotted as a function of z/L_θ, and that such effects on φ_h will be reduced.

The values of the Prandtl number, derived by Grachev et al. (2007b, Fig.1a) from the SHEBA data, show $Pr \approx 3$ for $Ri = 1$, and $Pr \approx 4$ for $Ri = 6$, in a tentative agreement with our values. The data displayed by Zilitinkevich et al. (2007, in their Fig. 1) indicate substantially different values, especially for larger *Ri*: $Pr \approx 3$ and $Rf \approx 0.3$ for $Ri = 1$, and $Pr \approx 30$ and $Rf \approx 0.4$ for $Ri = 6$.

4 Conclusions

Scaling of statistical moments of turbulence in stable conditions is not unique. Several scales of length, temperature and velocity can be formed on the basis of different moments of turbulence. Two gradient-based scaling sets, which employ variances and the potential temperature gradient, but do not include fluxes, have been considered, and verified through the use of empirical data.

Two composite datasets (referred to as *W* and *S*), obtained and described by Mahrt and (2006) Vickers based on CASES-99, are employed for this purpose. Case *W* is characterized by weak turbulence, small surface heat flux, and the local Richardson numbers exceeding the

critical value. In Case *S*, turbulence is stronger, and the local Richardson numbers are below the critical value.

The obtained figures indicate that the temperature-variance scaling (7) yields more consistent results. The resulting dimensionless moments approach constant values for sufficiently large values of the dimensionless height or *Ri*. This allows us to derive predictions for the Monin-Obukhov similarity functions φ_m and φ_h, the Prandtl number *Pr,* and the flux Richardson number *Rf* in terms of the local Richardson number *Ri*. A comparison of the derived expressions with other datasets gives ambiguous results due to substantial spread of observational data in very stable conditions.

Acknowledgments The performed research has been supported by the National Science Foundation grant No. ATM-0400590. The author's appreciation is directed to Drs. Larry Mahrt and Dean Vickers of Oregon State University for providing both datasets.

References

Balsley BB, Frehlich RG, Jensen ML, Meillier Y, and Muschinski A(2003) Extreme gradients in the nocturnal boundary layer: structure, evolution and potential causes. J. Atmos Sci 60: 2496-2508.

Brost RA, and Wyngaard JC (1978): A model study of the stably stratified planetary boundary layer. J Atmos Sci 36: 1041-1052.

Businger JA (1973) Turbulent transfer in the atmospheric surface layer. In: Workshop on Micrometeorology. Ed. D.A. Haugen. American Meteorological Society.

Chimonas H (1999) Steps, waves and turbulence in the stably stratified planetary boundary layer. Bound-Layer Meteor 90: 397-421.

Derbyshire SH and Wood N (1994) The sensitivity of stable boundary layers to small slopes and other influences. In: Stably Stratified Flows: Flow and Dispersion over Topography. Clarendon Press.

Duynkerke PG (1999) Turbulence, radiation and fog in Dutch stable boundary layers. Boundary-Layer Meteorol 90: 447-477.

Garrat JR and Brost RA (1981) Radiative cooling within and above the nocturnal boundary

layer. J Atmos Sci 38: 27-30-2746.

Grachev AA, Andreas EI, Fairall CW, Guest PS, Persson POG (2007a) SHEBA flux-profile relationship in the stable atmospheric boundary layer. Boundary-Layer Meteorol: 124, 315-333

Grachev AA, Andreas EI, Fairall CW, Guest PS, Persson POG (2007b) On the turbulent Prandtl number in the stable atmospheric boundary layer. Boundary-Layer Meteorol: 125, 329-341.

Ha K-J, Mahrt L (2003) Radiative and turbulent fluxes in the nocturnal boundary layer. Tellus 55A: 317-327.

Klipp C, Mahrt L (2004) Flux –gradient relationship, self-correlation and intermittency in the stable boundary layer. Quart. J Roy Meteorol Soc 130: 2087-2104.

Mahli YS (1995) The significance of the dual solutions for heat fluxes measured by the temperature fluctuation method in stable conditions. Boundary-Layer Meteorol 74: 389-396.

Mahrt L, Sun J, Blumen W, Delany T, and Oncley S (1998): Nocturnal Boundary-layer regimes. Bound-Layer Meteorol 88: 255-278.

Mahrt L (2003) Contrasting vertical structures of nocturnal boundary layers. Boundary-Layer Meteor 105: 351-363.

Mahrt L and Vickers D (2006) Extremely weak mixing in stable conditions. Boundary-Layer Meteorol 119 (1): 19-39.

Mahrt L (2007) The influence of nonstationarity on the turbulent flux-gradient relationship for stable stratification. Boundary-Layer Meteorol 125: 245-264.

Monin AS and Obukhov AM (1954) Basic laws of turbulence mixing in the surface layer of the atmosphere. Trudy Geof Inst AN SSSR 24 (151): 163-187.

Nappo CJ (1991) Sporadic breakdown of stability in the PBL over simple and complex terrain. Boundary-Layer Meteorol 54: 9-87.

Nieuwstadt FTM (1984) The turbulent structure of the stable, nocturnal boundary layer. J Atmos Sci 41: 2202 - 2216.

Oyha YD, Neff E, Meroney EN (1997) Turbulence structure in a stratified boundary layer under stable conditions. Boundary-Layer Meteorol 83: 139-161.

Poulos GS, Blumen W, Fritts DC, Lundquist JK, Sun J, Burns SP, Nappo C, Banta R, Newsom

R, Cuxart J, Terradellas E, Balsley BB, and Jensen ML (2002) CASES-99: A comprehensive investigation of the stable nocturnal boundary layer. Bull Amer Meteor Soc 83: 555-581.

Sorbjan Z *Structure of the Atmospheric Boundary Layer*. Prentice-Hall 1989 314 pp.

Sorbjan Z (1995) Self-similar structure of the planetary boundary layer. In: The Planetary Boundary Layer and Its Parameterization. 1995 Summer Colloquium. Ed.: C.-H. Moeng NCAR, 525 pp., Boulder, Colorado, USA.

Sorbjan Z (2006a) Local structure of turbulence in stably-stratified boundary layers. J Atmos Sci 63 (5): 526 1537.

Sorbjan Z (2006b) Comments on "Flux-gradient relationship, self-correlation and intermittency in the stable boundary layer". Quart J Roy Meteor Soc (July B) 130: 2087-2103

Sorbjan Z (2007a) Gradient-based similarity in the atmospheric boundary layer. Accepted by Acta Geophysica.

Van de Wiel BJH, Moene A, Hartogenesis G, De Bruin HA, Holtslag AAM (2003) Intermittent turbulence in the stable boundary layeor over land. Part III. A classification for observations during CASES-99. J Atmos Sci 60: 2509-2522.

Zilitinkevich SS, Elperin T, Kleeorin N, Rogachevskii I (2007) Energy- and flux budget (EFB) turbulence closure model for stably stratified flows. Part I: steady-state, homogeneous regimes. Boundary-Layer Meteorol: 125, 167-191

Figure Captions

Fig. 1. The gradient based scales as functions of height in Case *S* (strong turbulence) and Case *W* (weak turbulence): (a) the length scales L_w and L_θ, (b) the temperature scales T_w, and T_θ, (c) the velocity scales U_w, and U_θ.

Fig. 2. The dependence of the dimensionless moments on the Richardson number *Ri* in case *S* (black circles and black squares) and case *W* (grey circles and gray squares): (a) the dimensionless heat fluxes $\overline{w\theta}/(U_w T_w)$ and $\overline{w\theta}/(U_\theta T_\theta)$, (b) the dimensionless momentum fluxes $\overline{uw}/U_w^2$ and $\overline{uw}/U_\theta^2$, (c) the dimensionless variances $\overline{\theta^2}/T_w^2$ and $\overline{w^2}/U_\theta^2$.

Fig. 3. Dependence between the dimensionless parameter z/L_θ on the Richardson number *Ri* in Case *S* (black circles) and Case *W* (grey circles). The marked curve is described by the equation $z/L_\theta = 25\ Ri^{0.6}$.

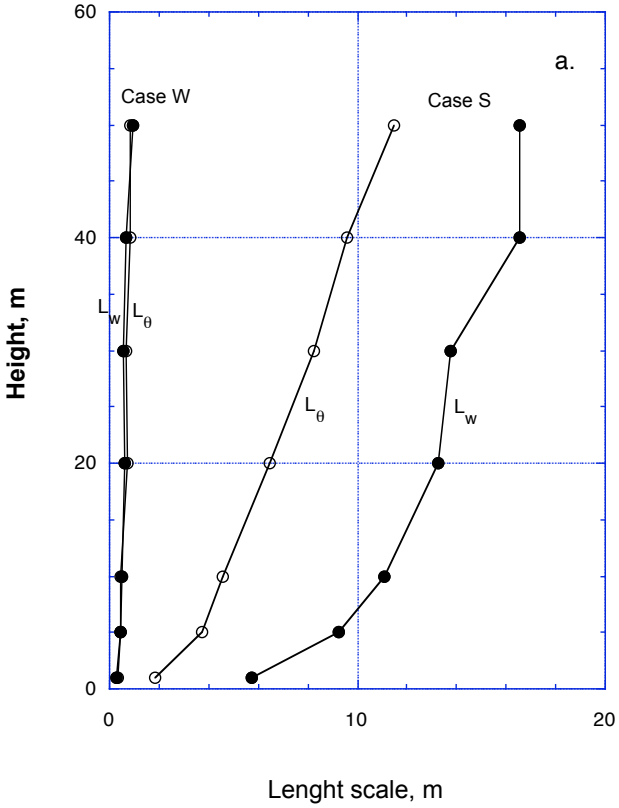
a.
Case W
Case S
L_w
L_θ
L_θ
L_w
Height, m
Lenght scale, m
0
20
40
60
0
10
20

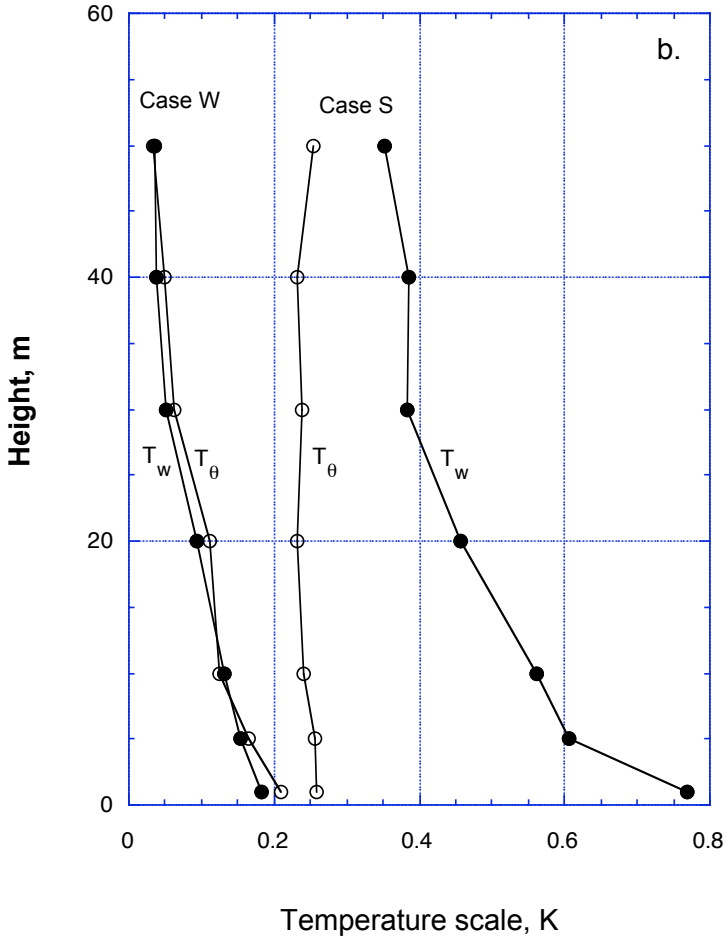
b.
Case W
Case S
T_w
T_θ
T_θ
T_w
Height, m
60
40
20
0
0
0.2
0.4
0.6
0.8
Temperature scale, K

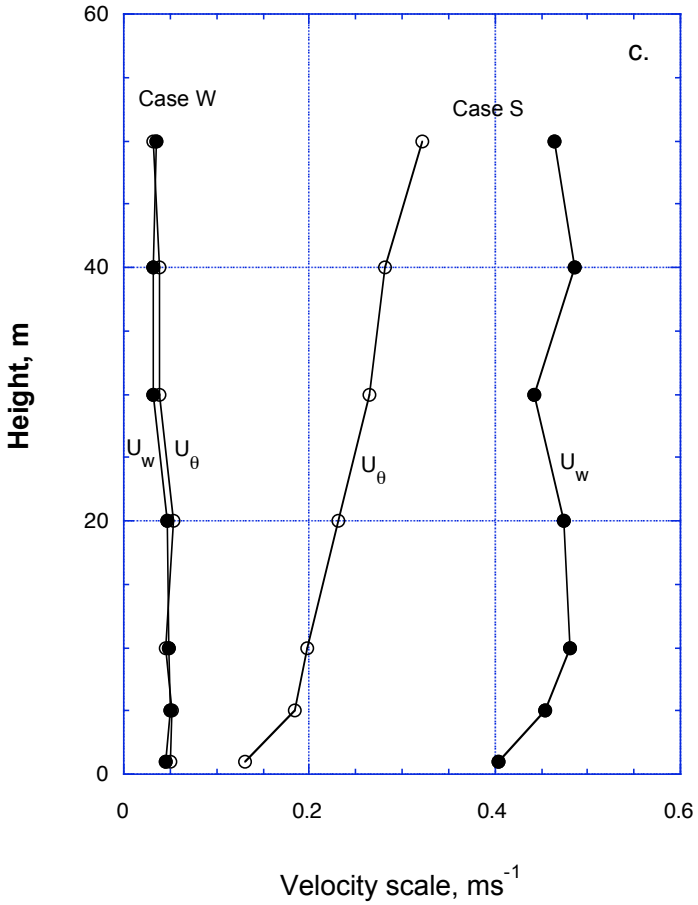
c.
Case W
Case S
Height, m
60
40
20
0
0
0.2
0.4
0.6
U_w
U_θ
U_θ
U_w
Velocity scale, ms^{-1}

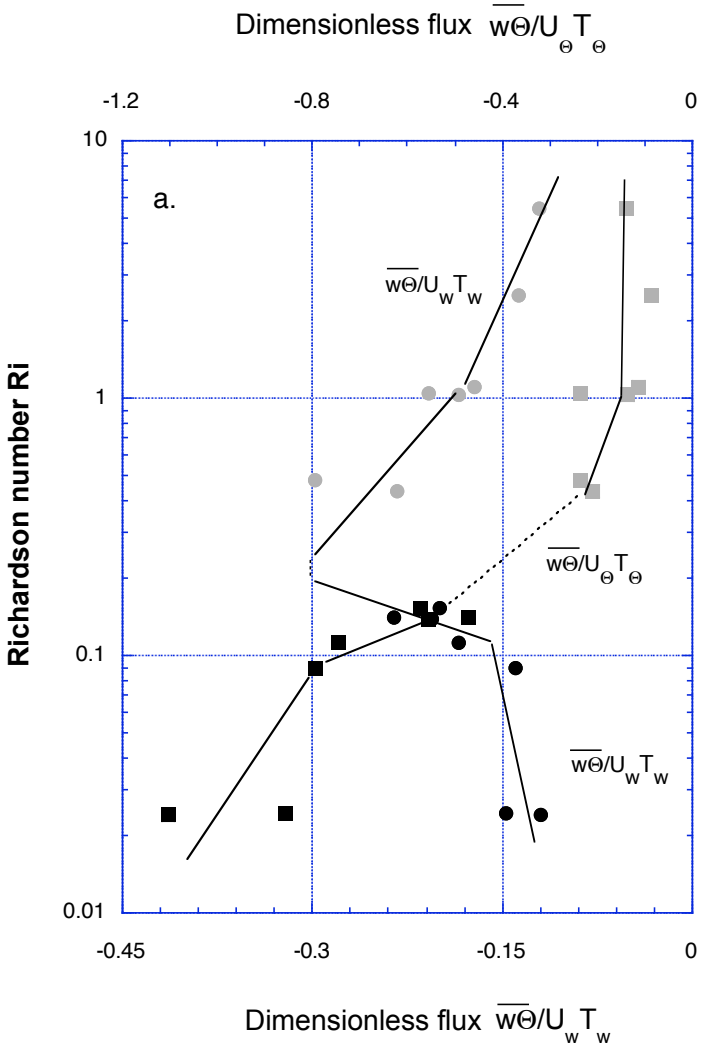
Dimensionless flux $\overline{w\Theta}/U_\Theta T_\Theta$
-1.2
-0.8
-0.4
0
10
1
0.1
0.01
a.
$\overline{w\Theta}/U_w T_w$
$\overline{w\Theta}/U_\Theta T_\Theta$
$\overline{w\Theta}/U_w T_w$
Richardson number Ri
-0.45
-0.3
-0.15
0
Dimensionless flux $\overline{w\Theta}/U_w T_w$

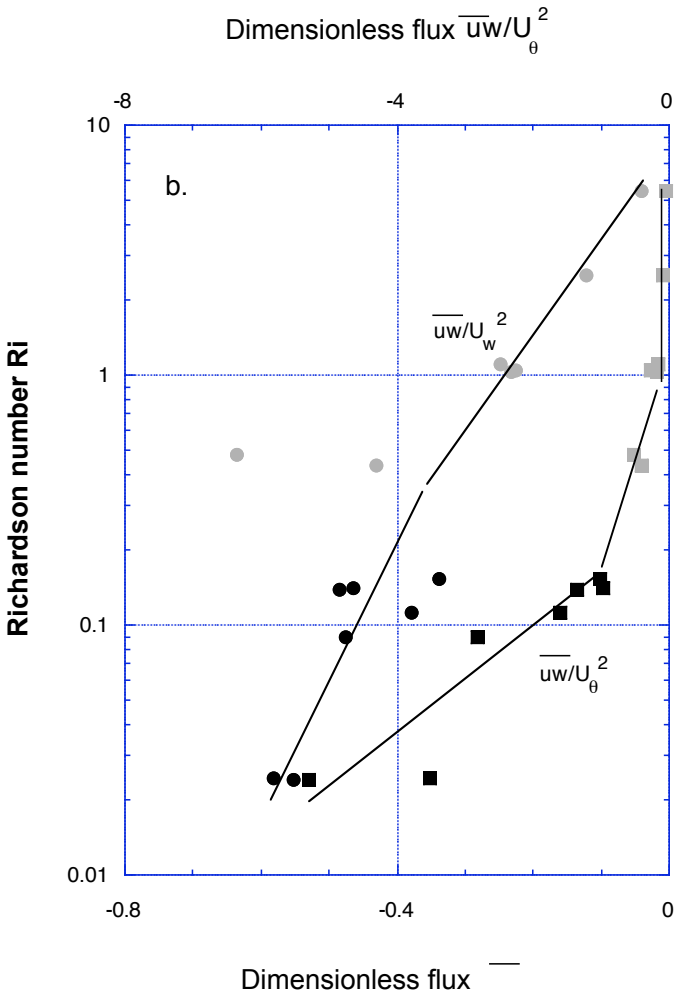
Dimensionless flux $\overline{uw}/U_\theta^2$
-8
-4
0
10
1
0.1
0.01
b.
$\overline{uw}/U_w^2$
$\overline{uw}/U_\theta^2$
Richardson number Ri
-0.8
-0.4
0
Dimensionless flux

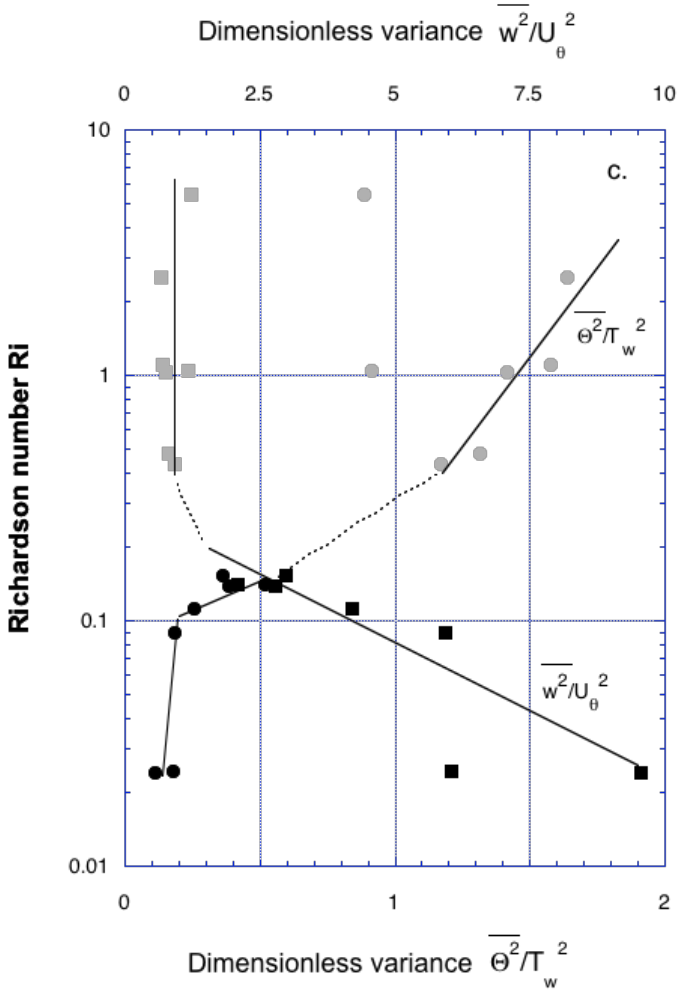
Dimensionless variance $\overline{w^2}/U_\theta^2$
0
2.5
5
7.5
10
10
1
0.1
0.01
c.
$\overline{\Theta^2}/T_w^2$
$\overline{w^2}/U_\theta^2$
Richardson number Ri
0
1
2
Dimensionless variance $\overline{\Theta^2}/T_w^2$

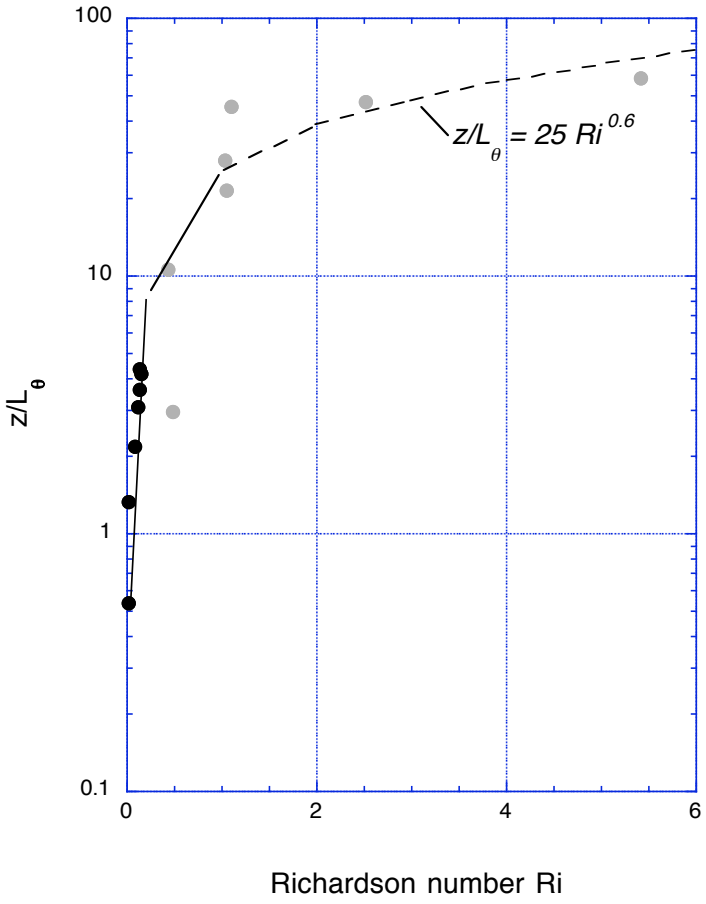
100
10
1
0.1
0
2
4
6
z/L_θ
z/L_θ = 25 Ri^0.6
Richardson number Ri